Surface Reaction of 1,2,-Dichloroethylene on Si(100)-2 × 1: Importance of Surface Isomerization Channel

ARTICLE *in* THE JOURNAL OF PHYSICAL CHEMISTRY C · JANUARY 2008

Impact Factor: 4.77 · DOI: 10.1021/jp076526o

4 AUTHORS, INCLUDING:

Manik Ghosh
University of Limerick
26 PUBLICATIONS **167** CITATIONS
SEE PROFILE

Majher Ibna Mannan Sarker
Marquette University
7 PUBLICATIONS **31** CITATIONS
SEE PROFILE

Cheol Ho Choi
Kyungpook National University
111 PUBLICATIONS **2,117** CITATIONS
SEE PROFILE

Surface Reaction of 1,2,-Dichloroethylene on Si(100)-2 × 1: Importance of Surface Isomerization Channel

Manik Kumer Ghosh, Majher Ibna Mannan Sarker, and Cheol Ho Choi*

Department of Chemistry, College of Natural Sciences, Kyungpook National University, Taegu 702-701, South Korea

Received: August 14, 2007; Revised Manuscript Received: January 20, 2008

The surface reactions of *trans*-1,2-dichloroethylene (DCE) on Si(100)-2 × 1 were theoretically investigated to study the effects of chlorine substitutions on surface reactions. As in the case of pristine ethylene, diradical as well as π-complex channels leading to [2 + 2] cycloaddition products were found. In general, chlorine substitution makes the former kinetically more favorable and also changes its stereochemistry. In addition to modifying those existing reaction channels, the chlorine substitution opens new subsequent low-energy pathways leading to the experimentally suggested mono- and dichlorinated adstructures. Their large stabilities with low kinetic barriers make them the major surface species. Current study demonstrates that substitutions not only have large effects on existing reaction channels, but also introduces new possibilities, significantly changing the overall surface reactions.

I. Introduction

[2_s+2_s] cycloadditions are formally orbital symmetry forbidden,[1] expecting a large reaction barrier along the symmetric reaction pathway. However, the rules governing [2 + 2] additions on the Si(100)−2 × 1 surface have been shown to be apparently different. Early experimental[2] and theoretical[3] studies have shown that ethylene, propylene, and acetylene easily chemisorb on Si(100)−2 × 1 yielding [2 + 2] products and are able to resist temperatures of up to 600 K. Consequently, it is now a general consensus that the formally symmetry-forbidden[1] [2 + 2] cycloaddition reactions of alkynes and alkenes on the Si(100) surface easily occur.[4]

However, the exact nature of surface [2 + 2] cycloaddition mechanisms is still under active discussion. In addition, the substitution effects have been largely unexplored except for some limited reaction channels.[5] The two most likely reaction pathways are π-complex and diradical channels (see Scheme 1). The π-complex channel can be described by a three-atom intermediate, which was proposed for acetylene adsorption on Si(100).[6] With the help of IR experiments, Liu and Hamers[7] reported that the adsorption of *cis*- and *trans*-1,2-dideuterioethylene on Si(100) is stereospecific and therefore should follow a π-complex channel. In contrast, based on STM (scanning tunneling microscopy) results, Lopinski et al.[8] suggested that the surface reaction of *trans*-2-butene on Si(100) is not stereospecific but 98% stereoselective with a small degree of isomerization, indicating that the reaction follows a diradical pathway. Theoretically, with the help of the B3LYP functional,[9] Lu[10] and co-workers concluded that, although the overall reaction is not stereospecific, it still would show high sterose-lectivity in accord with the STM experiment.[8]

Although it may be reasonable to assume that ethylene and its dimethyl-substituted derivative (2-butene) behave similarly on the Si(100) surface regarding the [2 + 2] cycloaddition, the possibility that 2-butene undergoes alternative reaction pathways due to the presence of the two methyl groups cannot be ruled out. In fact, in a comparative study of ethylene and 2-butene on the Si(100)−2 × 1 surface, Lee et al.[11] showed that a significantly different reaction channel exists in the 2-butene surface reaction on Si(100), in which a methyl hydrogen easily transfers to the surface via the ene reaction.[12] The possibility of new reaction channels of the substituted unsaturated system was also reported by Leung and co-workers[13] who experimentally showed that dichloroethylene and perchloroethylene upon adsorption on the Si(100)−2 × 1 surface undergo an insertion reaction instead of the expected [2 + 2] cycloaddition reaction. They suggested both triatom π-complex and diradical intermediate pathways as possible reaction channels. However, the exact nature of the insertion reaction is not certain.

SCHEME 1

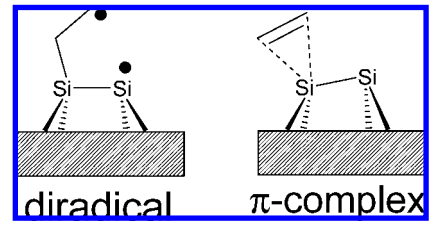

These studies suggest that substituents can perturb the existing potential energy surfaces to the degree that they become a major factor in the surface adsorption reactions. Thus, in addition to the well-known pathways, exploring possibilities of alternative channels is equally important. In this paper, the surface reaction mechanisms of *trans*-1,2-dichloroethylene (DCE) on Si(100)−2 × 1 were theoretically explored in order to elucidate the nature of the reactions as observed in experiments especially focusing on the substitution effects.[13]

II. Computational Details

Design of SIMOMM models. In order to study surface size effects, a hybrid quantum mechanics/molecular mechanics (QM/MM) method called SIMOMM[14] (surface integrated molecular orbital molecular mechanics) was used. This approach embeds a smaller QM cluster in a much larger MM cluster in order to

* cchoi@knu.ac.kr.

10.1021/jp076526o CCC: $40.75
Published on Web 05/29/2008

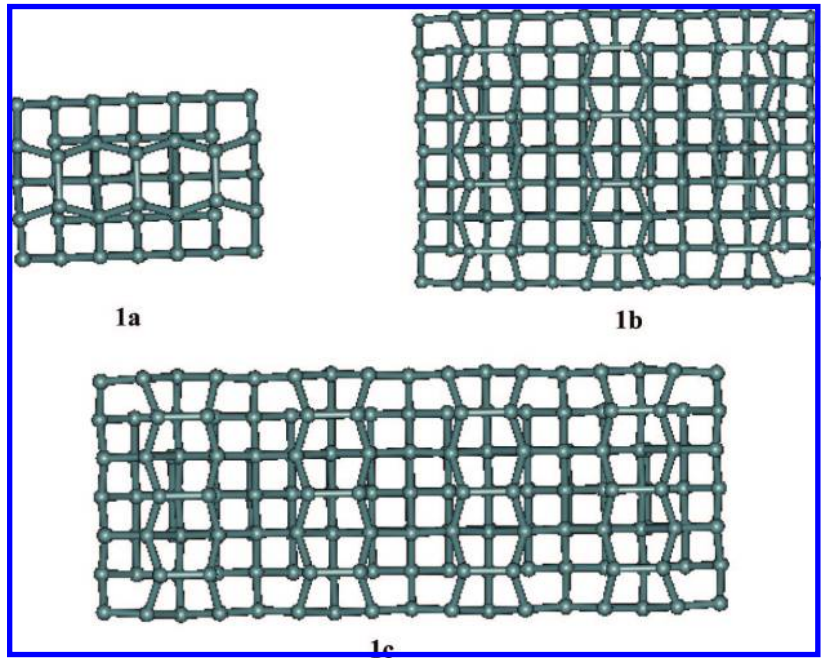

Figure 1. Bulk SIMOMM models for single dimer (a), along the dimer row (b), and across dimer row (c) calculations in this study.

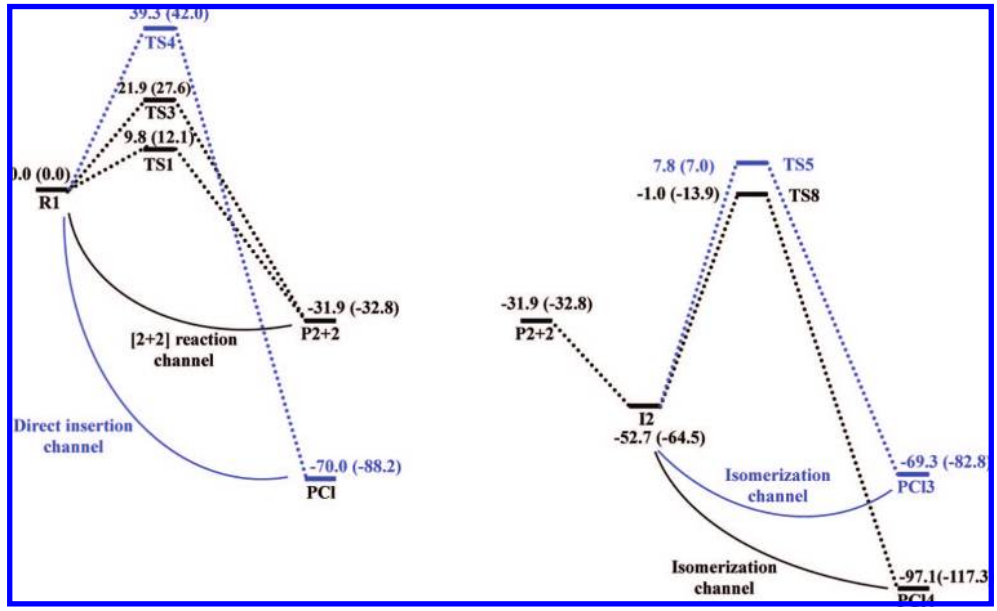

Figure 2. The potential energy surfaces (PES) along the [2 + 2] cycloaddition channel, direct insertion channel, indirect isomerizations.

reduce or eliminate possible edge effects. Three different SIMOMM models were designed in this work (see Figure 1). Figure 1a represents a $C_2Cl_2Si_9H_{14}$ quantum region embedded in a $C_2Cl_2Si_{48}H_{38}$ cluster for single dimer calculations. This bulk model of silicon surface includes three dimers. Figure: 1b represents a $C_2Cl_2Si_{15}H_{18}$ quantum region embedded in a $C_2Cl_2Si_{196}H_{94}$ cluster for the adsorptions along the dimer rows. The bulk model of silicon surface includes 12 dimers, being 3 dimer rows wide by 4 dimers long. Figure 1c represents a $C_2Cl_2Si_{20}H_{24}$ quantum region embedded in a $C_2Cl_2Si_{186}H_{98}$ cluster for the adsorptions across the dimer rows. The bulk model of silicon surface includes 12 dimers, being 4 dimer rows wide by 3 dimers long. MM3[15] parameters were used for the molecular mechanics optimization part of the computations.

Design of Basis Sets. Two basis sets were used throughout this work. The all-electron 6−31G(d)[16] basis set was used for smaller clusters **1a**. The Hay-Wadt[17] effective core potential with polarization functions was used for larger clusters **1b** and **1c**. This basis set is referred to as HW(d).

Design of CASSCF Active Spaces. Various points on the reaction paths, particularly transition states and intermediates, are often inherently multiconfigurational as shown by previous studies.[18] Therefore, CASSCF (complete active space SCF) wave functions[19] were used to describe entire potential energy surfaces. For the single dimer, an (8,8) active space was used, which is constructed from four electrons of the π, π^*, σ, and σ^* orbitals of surface silicon dimer, plus two electrons of the π and π^* orbitals of the C−C bond and two electrons of the σ and σ^* orbitals of the C−Cl bond. For the along dimer row calculations, a (12,12) active space was used, which is constructed from four electrons of the π and π^* orbitals of two silicon dimers and two electrons of the π and π^* orbitals of the C−C bond, plus two electrons from σ and σ^* of surface one silicon dimer and four electrons from the σ and σ^* orbitals of

CHART 1: CASSCF Transition States and Intermediates along the Diradical Channel Using SIMOMM Model 1a[a]

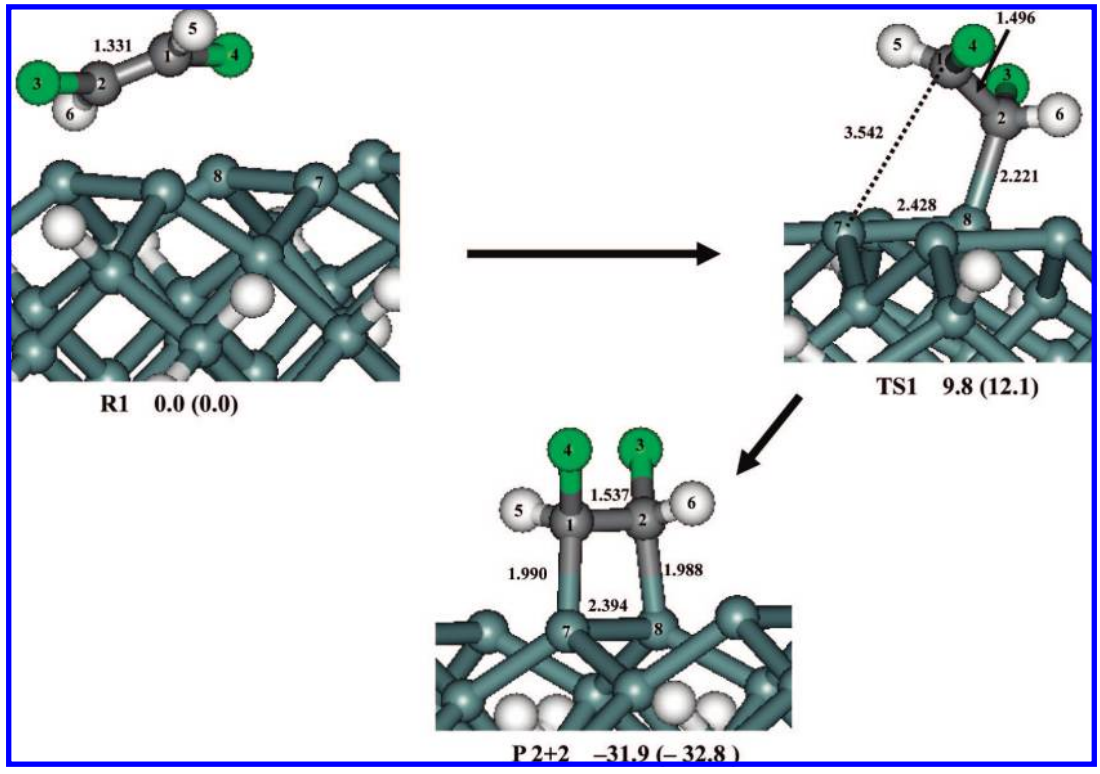

[a] Relative energies are obtained with SIMOMM:MRMP2(8,8)/6-31G(d). The values in parentheses are obtained with SIMOMM:CASSCF(8,8)/6-31G(d). Geometric data are from the CASSCF results.

CHART 2: Transition States and Intermediates of the π-Complex Channel Using SIMOMM Model 1a[a]

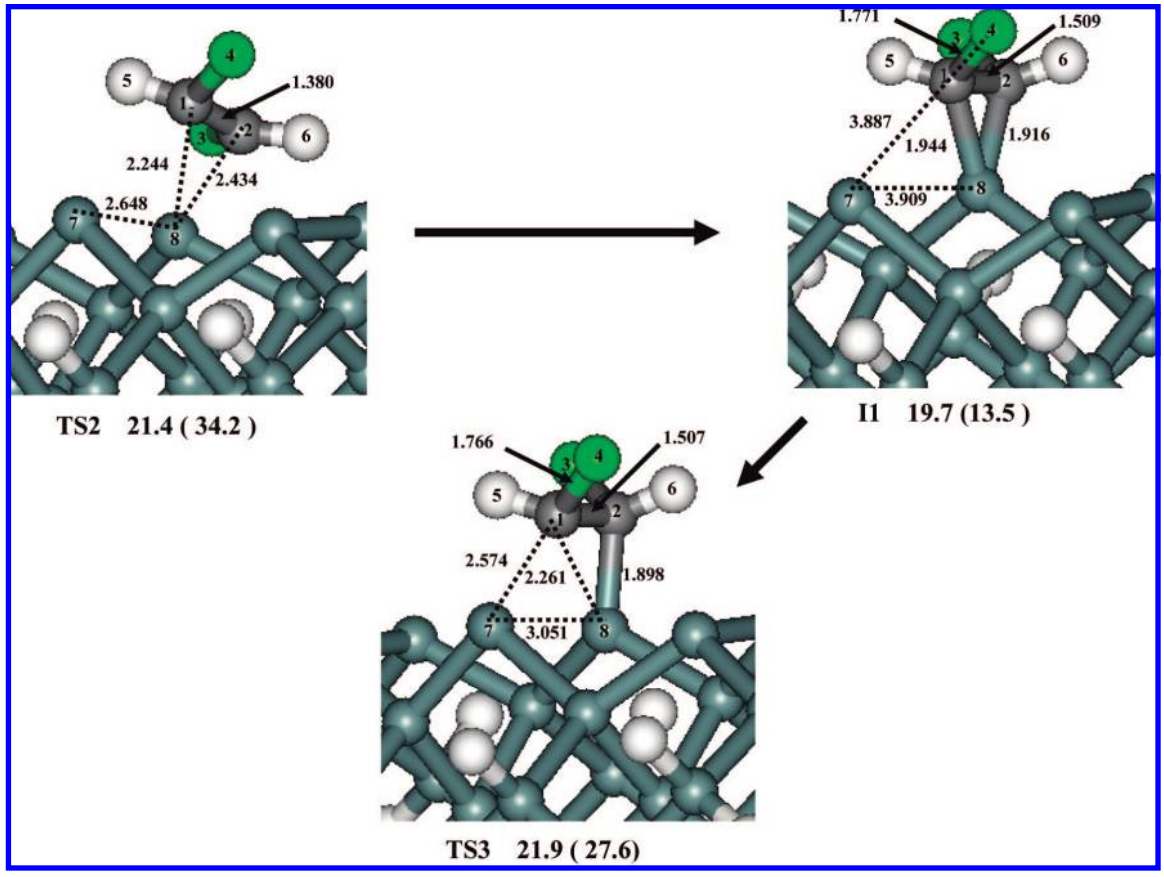

[a] Relative energies are obtained with SIMOMM:MRMP2(8,8)/6-31G(d). The values in parentheses are obtained with SIMOMM:CASSCF(8,8)/6-31G(d). Geometric data are from the CASSCF results.

CHART 3: CASSCF Transition States and Intermediates along the Direct Insertion Channel Using SIMOMM Model 1a[a]

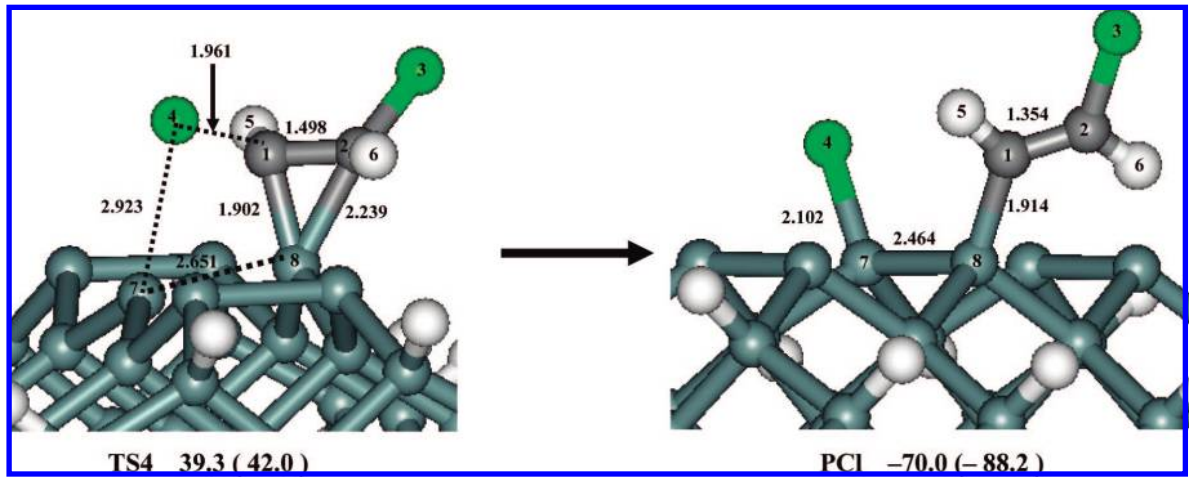

[a] Relative energies are obtained with SIMOMM:MRMP2(8,8)/6-31G(d). The values in parentheses are SIMOMM:CASSCF(8,8)/6-31G(d). Geometric data are from the CASSCF results.

CHART 4: CASSCF Transition States and Intermediates along the Second Direct Insertion Channel Using SIMOMM Model 1a[a]

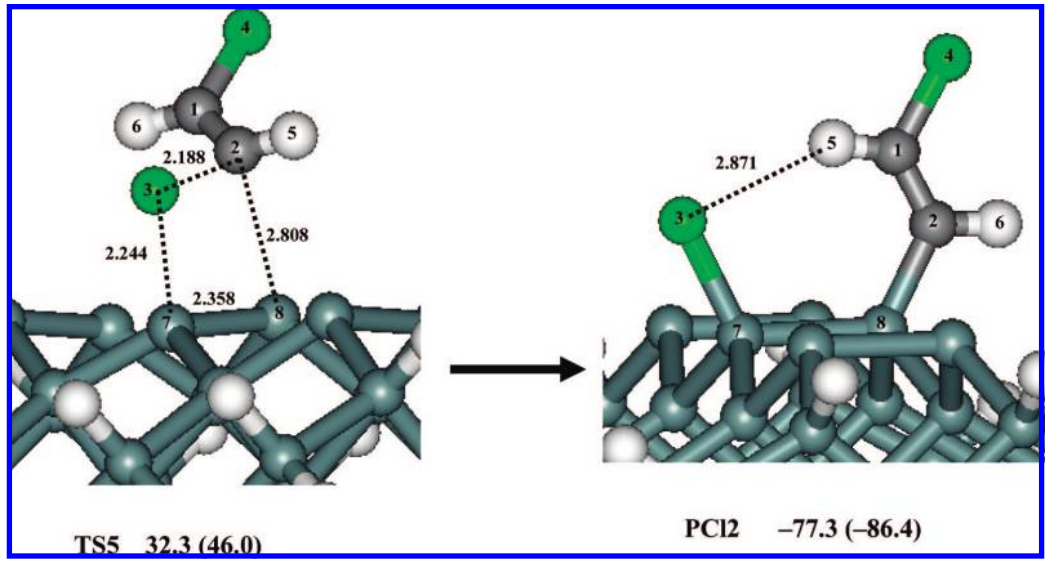

[a] Relative energies are obtained with SIMOMM:MRMP2(8,8)/6-31G(d). The values in parentheses are obtained with SIMOMM:CASSCF(8,8)/6-31G(d). Geometric data are from the CASSCF results.

the two C−Cl bonds. For the across dimer row calculations, a (6,6) active space wave function was constructed including four electrons of π and π^* orbitals of two silicon dimers plus two electrons of the π and π^* orbitals of the C−C bond.

In order to recover the dynamic electron correlation, and to ensure that all parts of the reaction path are treated equivalently, multireference second-order perturbation theory was used, since the level of accuracy for such methods is at least comparable to that of MP2 when single reference methods are appropriate.[20] The particular version of this method used in the present work is referred to as MRMP2 (multireference second order perturbation theory).[21] The GAMESS (general atomic and molecular electronic structure system)[22] program was used for all of the computations. Minimum energy reaction paths were determined by first optimizing the geometries of the minimum and the transition states. The Hessian matrix (matrix of energy second derivatives) was computed and diagonalized for all stationary points to characterize them.

All of the computations were done without imposing symmetry unless otherwise specified.

III. Discussions

Potential energy surface searches yielded both [2 + 2] reaction products and chlorinated products. They shall be discussed in order. All geometries and energies were obtained with CASSCF and MRMP2 theories, respectively. The overall energetics along the potential energy surfaces are collected in Figure 2.

A. [2 + 2] Reaction Channels on Single Dimer. ***Diradical Channel.*** Simple diradical channels were found (see Chart 1). In contrast to the pristine ethylene diradical channel,[11] only one transition state **TS1** exists along the reaction pathway, directly connecting the reactants (the bare surface and DCE) and the [2 + 2]cycloaddition product, **P2 + 2**. The radical character of **TS1** can be easily seen from the NOON (natural orbital occupation number) values of CASSCF active space, which are

CHART 5: CASSCF Transition States and Intermediates along the Isomerization Channel Using SIMOMM Model 1a[a]

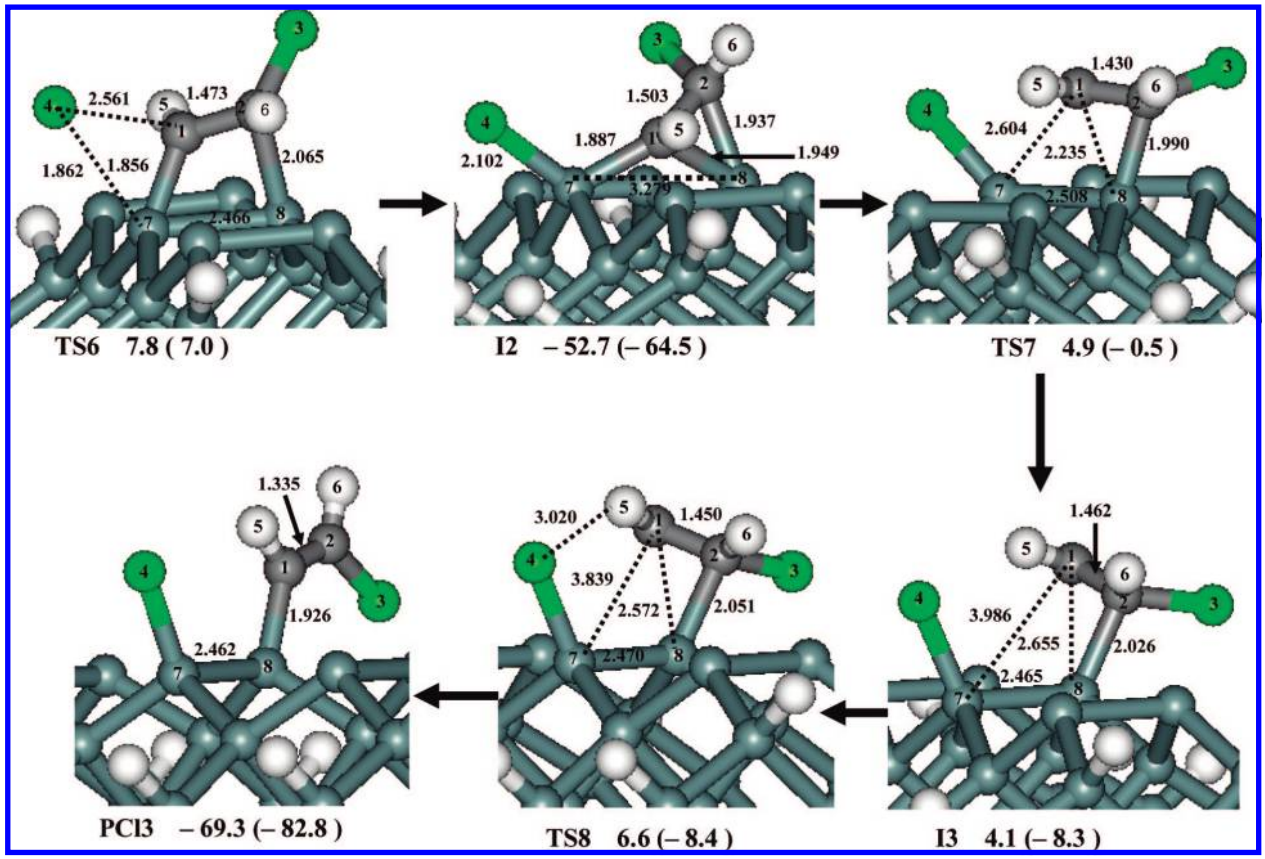

[a] Relative energies are obtained with SIMOMM:MRMP2(8,8)/6-31G(d). The values in parentheses are SIMOMM:CASSCF(8,8)/6-31G(d). Geometric data are from the CASSCF results.

CHART 6: CASSCF Transition States and Intermediates along the Second Isomerization Channel Using SIMOMM Model 1a[a]

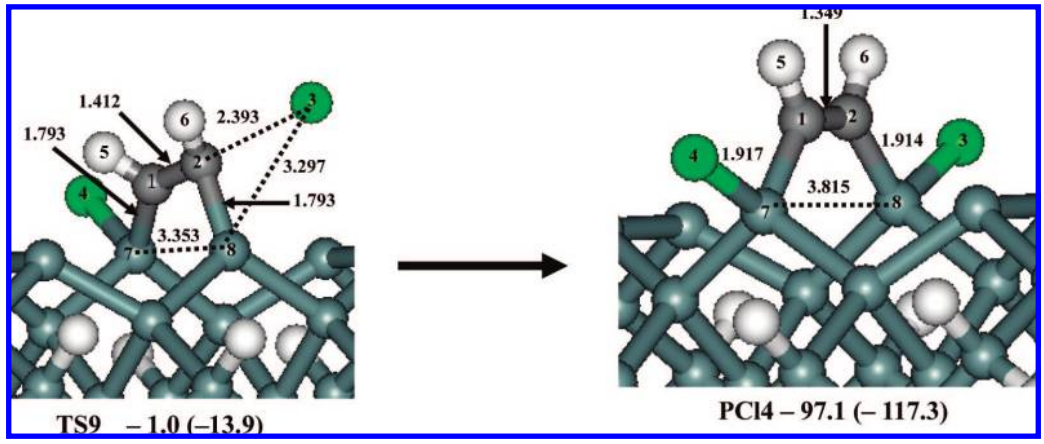

[a] Relative energies are obtained with SIMOMM:MRMP2(8,8)/6-31G(d). The values in parentheses are SIMOMM:CASSCF(8,8)/6-31G(d). Geometric data are from the CASSCF results.

1.983, 1.972, 1.970, 1.024, 0.976, 0.028, 0.026, and 0.017. As a result of one transition path, there is no chance of internal rotation around the C═C bond, making the current path stereospecific. In the case of the diradical path of pristine ethylene, a mono-σ bonded intermediate exists allowing internal rotations around C═C bond. The reaction barrier of **TS1** is calculated to be 9.8 kcal/mol, which is 2.5 kcal/mol lower than the overall barrier of the pristine ethylene diradical channel. The reduced barrier height may be due to the strong electronegativity of chlorine atoms that weaken the π-bond of C═C bond so that the diradical formation during the transition state can be stabilized. Accordingly, the substituted chlorine atoms not only simplify the initial adsorption pathway but also reduce the reaction barrier affecting the kinetic aspect of the diradical channel significantly.

The [2 + 2]cycloaddition product, **P2** + **2**, is more stable than the reactants by 31.9 kcal/mol at the MRMP2 level of theory, which is similar to that of pristine ethylene (33.0 kcal/mol), showing that the chlorine substitution has relatively little effect on thermodynamics of the diradical channel.

π-Complex Channel. As in the cases of ethylene[11] and acrylonitrile adsorptions,[23] a π-complex channel leading to the

CHART 7: [2 + 2] Cycloaddition Reactions on Single Dimer Using Two Dimer Model 1b[a]

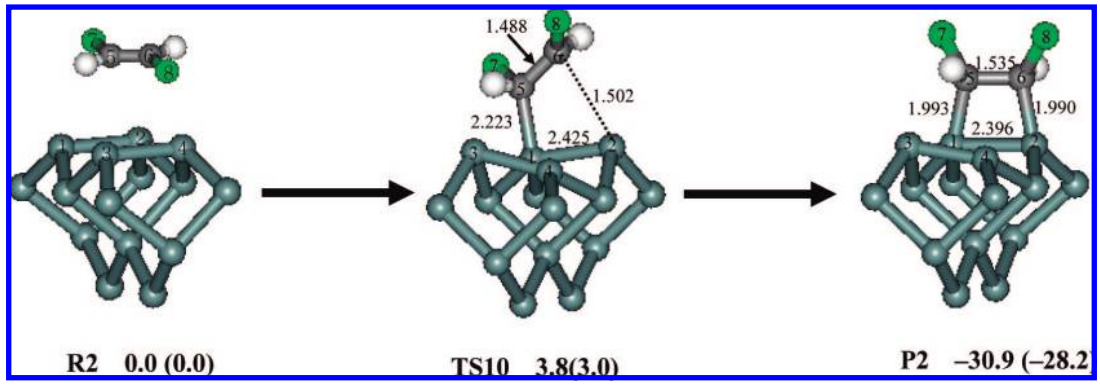

[a] Relative energies are obtained with SIMOMM:MRMP2(12,12)/HW(d). The values in parentheses are obtained with SIMOMM:CASSCF(12,12)/HW(d). Geometric data are from the CASSCF results.

[2 + 2] product was also found (Chart 2). In this channel, the initial transition state **TS2** connects the reactants and a π-complex intermediate **I1** with a barrier of 21.4 kcal/mol. The intermediate **I1** is endothermic by 19.7 kcal/mol as compared to the reactants. The next transition state **TS3** connects **I1** and the [2 + 2] product, **P2** + **2**, with a barrier of 21.9 kcal/mol. The corresponding overall barriers of ethylene and acrylonitrile π-complex channels were calculated to be 17.0 and 16.7 kcal/mol, respectively. Therefore, it is seen that substituted chlorine atoms increase the reaction barrier of the π-complex channel. This may be due to the fact that the electronegative chlorine atoms reduce π-electron donations of C═C to the surface silicon. According to the MRMP2 results, overall potential energy surfaces are quite flat as was also observed in the case of ethylene. Since the two carbon atoms are bound to one surface silicon atom in **I1**, there is essentially no chance of internal rotation around the C1−C2 bond. Therefore, the stereochemistry of initial reactants is stereospecifically retained.

Overall, the chlorine substitution shows contrasting kinetic effects on diradical and π-complex channels. While it facilitates the diradical path, the same substitution hinders the π-complex channel, making the already preferred diradical path more favorable between the two.

B. Chlorination Channel on Single Dimer. The above two known channels are not consistent with the experimental results[13] where the surface Si−Cl adstructures were found. Therefore, the possibilities of C−Cl bond activations were further explored, yielding new reaction pathways.

Direct Insertion Channel. According to our calculations, a reaction competition between the π-complex explained above and a new direct insertion channel exists from the intermediate **I1** of the π-complex channel. Instead of **TS3**, a new insertion transition state **TS4** (see Chart 3) in which the Si7−Si8 bond and Si7−Cl4 bond are formed while the C1−Cl4 bond is broken, directly connecting the **I1** and a monochlorinated product, **PCl** with a large barrier of 39.3 kcal/mol. The barrier of **TS4** is higher than that of **TS3** by 17.4 kcal/mol, making this direct insertion path from the intermediate **I1** kinetically less favorable than the π-complex channel. However, the product of direct insertion channel **PCl** is thermodynamically more stable than the [2 + 2] cycloaddition product, **P2** + **2** by 38.1 kcal/mol.

In another channel (see Chart 4), an insertion transition state **TS5** in which Si8−C2 and Si7−Cl8 bonds are formed, while the C2−Cl3 bond is broken, directly connects the reactant **R** and the monochlorinated product **PCl2** with a barrier height 32.3 kcal/mol which is 7.0 kcal/mol lower than the former channel. However, the barrier of **TS5** is still much higher than those of [2 + 2] cycloaddition channels.

In short, although the direct insertion channel produces a thermodynamically more stable product, it cannot be the major channel due to the large kinetic barrier.

Isomerization Channels. In addition to the direct insertion channels, low-energy C−Cl bond activation paths were found. Theses are particularly called as isomerizations, since the starting point of this channel is the well-known [2 + 2] surface product **P2** + **2**. By transferring a chlorine atom Cl4 from C1 to Si7, the transition state **TS6** (see Chart 5) connects the initial [2 + 2] product **P2** + **2** and an intermediate **I2**. The calculated reaction barrier of **TS7** is 7.8 kcal/mol, which is lower than the **TS1** reverse reaction barrier from [2 + 2] product. Therefore, the isomerization reaction is preferred between the two possible reactions from **P2** + **2**. The chlorine transfer breaks the Si7−Si8 surface bond yielding an interesting new surface species **I2**, which has not been previously suggested. It is noted that Si7, Si8, C1, and C2 are all tetra-coordinated in **I2**, yielding a thermodynamically very stable adstructure that is more stable than the [2 + 2] product **P2** + **2** by 20.8 kcal/mol.

By forming a Si7−Si8 bond and breaking Si7−C1 and Si8−C1 bonds, a subsequent transition state **TS7** connects the stable intermediate **I2** and a diradical intermediate **I3**. The reaction barrier of **TS7** is 4.9 kcal/mol, which is lower than the previous transition state **TS6** by 2.9 kcal/mol. Because of its diradical nature, the intermediate **I3** is not thermodynamically stable. In fact, it is less stable than the reactants by 4.1 kcal/mol. By shifting the Si8 from C2 to C1, a transition state **TS8** connects **I3** and a monochlorinated product **PCl3**, which is a rotational isomer of **PCl** with respect to the C1═C2 bond. They are nearly identical in energy. The transition state **TS8** has a small reaction barrier of 6.6 kcal/mol, which is again lower than **TS6** by 1.2 kcal/mol. As a result, the overall reaction barrier is lower than all three channels discussed earlier making this path kinetically the most favorable. Furthermore, the resultant monochlorinated **PCl3** surface product is thermodynamically much more stable than the [2 + 2] product. Therefore, it is expected that once the [2 + 2] product is formed, it would be converted into **PCl3** very easily.

The stable intermediate **I2** is again a starting point for another path leading to the most stable dichlorinated surface species-.(Chart 6). In order to study this part of the potential energy surface, the C2−Cl3 σ and σ^* orbitals was used instead of those of Si7−Cl4 for the (8,8) active space. By transferring the Cl3 from C2 to Si8, the **TS9** connects **I2** and the most stable dichlorinated adstructure **PCl4**. The reaction barrier of **TS9** is

CHART 8: [2 + 2] Cycloaddition Reactions along the Dimer Row Using Two Dimer Model 1b[a]

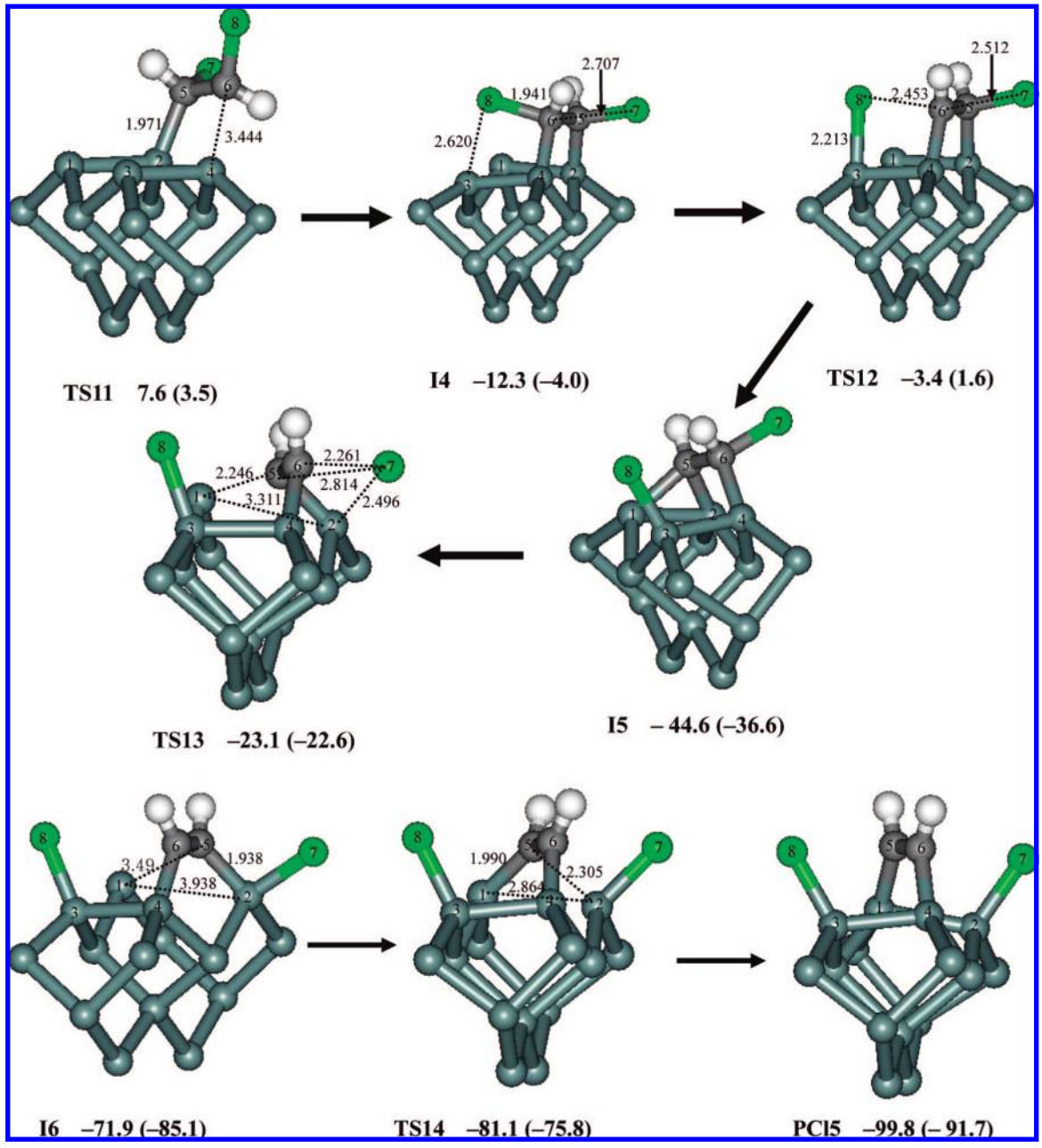

[a] Relative energies are obtained with SIMOMM:MRMP2(12,12)/HW(d). The values in parentheses are obtained with SIMOMM:CASSCF(12,12)/HW(d). Geometric data are from the CASSCF results.

−1.0 kcal/mol, which is lower than that of **TS7** by 5.9 kcal/mol. Therefore, although there is a reaction competition between **PCl3** and **PCl4**, the isomerization reaction leading to the dichlorinated **PCl4** is kinetically slightly more favorable. Furthermore, the dichlorinated **PCl4** is 27.8 kcal/mol more stable than the monochlorinated **PCl3**. Consequently, the dichlorinated adstructure formation path is both kinetically and thermodynamically more favorable than those to monochlorinated adstructures. Since the reaction barriers leading to the mono- and dichlorinated products are lower than the diradical and the π-complex [2 + 2] cycloaddition paths, once [2 + 2] cycloaddition product **P2 + 2** is formed, it would soon be thermally redistributed to the more stable **PCl3** and **PCl4**, of which the latter is preferred over the former both kinetically and thermodynamically. This theoretical conclusion that the chlorinated products are the major surface species is consistent with the experimental observations.[13]

In short, the chlorinated adstructures are formed via *indirect* isomerization reactions after forming the initial [2 + 2] cycloaddition products. It is found that such isomerizations have very low reaction barriers and the resulted chlorinated adstructures are thermodynamically much more stable than the [2 + 2] product. Due to the lower reaction barriers of subsequent surface reactions as compared to the initial adsorptions, the overall surface reactions become thermodynamically controlled, contrasting with the kinetically controlled surface reactions found in pristine ethylene adsorption.[11]

Since the *indirect* isomerizations are the major channels, the [2 + 2] cycloaddition adsorptions along and across the dimer rows were mainly investigated for the two possible dimer reactions in the following sections.

C. Adsorptions along the Dimer Rows. For the study of adsorptions along the dimer row, SIMOMM model **1b** was used in combination with (12,12) active space and HW(d) basis sets.

CHART 9: [2 + 2] Cycloaddition Reactions on Single Dimer Using Two Dimer Model 1c[a]

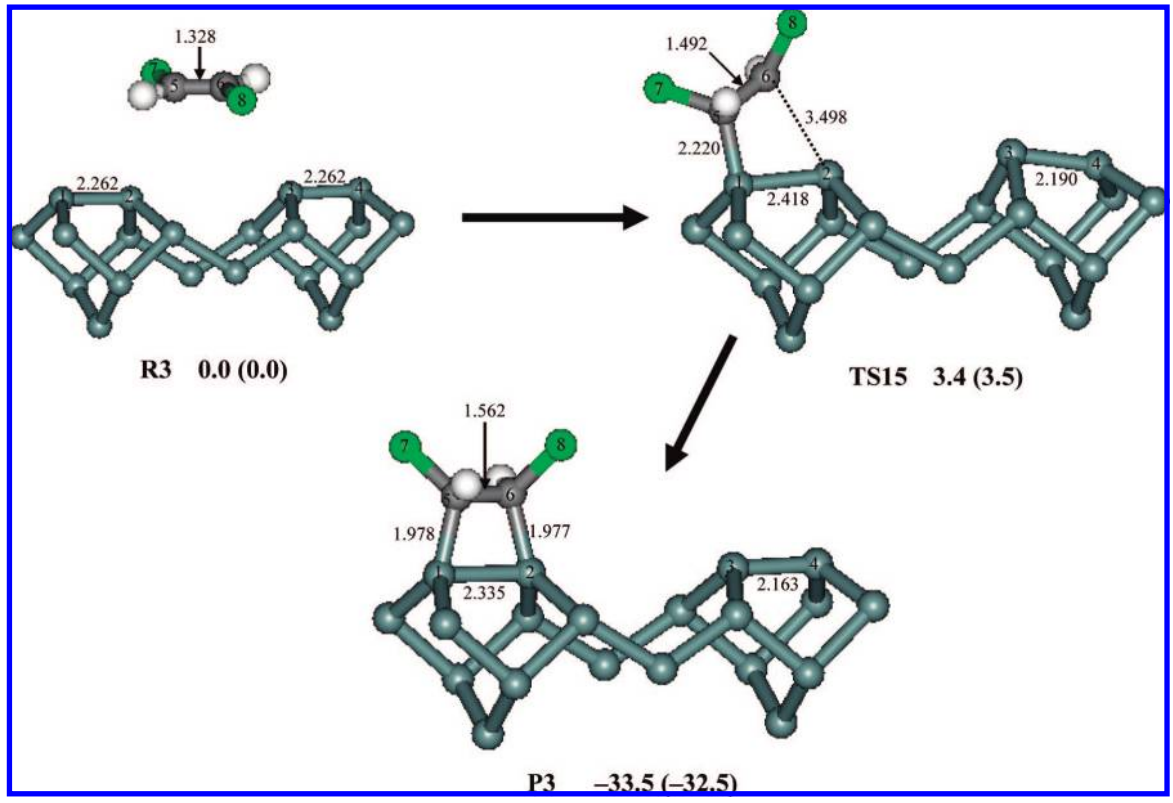

[a] Relative energies are obtained with SIMOMM:MRMP2(6,6)/HW(d). The values in parentheses are obtained with SIMOMM:CASSCF(6,6)/HW(d). Geometric data are from the CASSCF results.

CHART 10: [2 + 2] Cycloaddition Reactions Across the Dimer Row Using Two Dimer Model 1c[a]

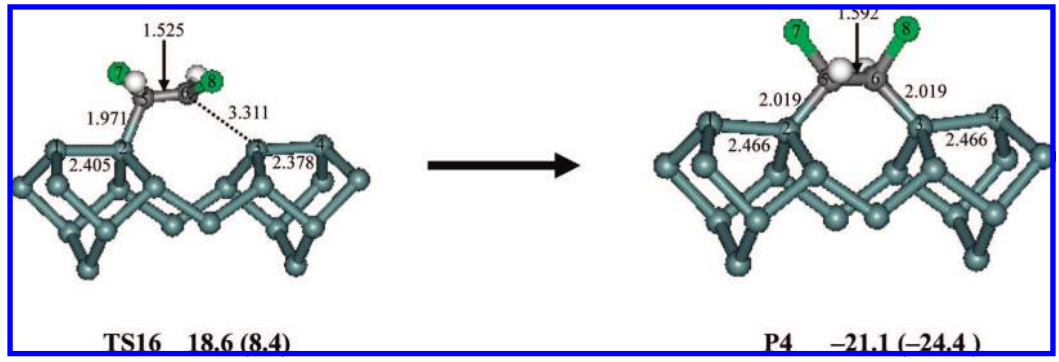

[a] Relative energies are obtained with SIMOMM:MRMP2(6,6)/HW(d). The values in parentheses are obtained with SIMOMM:CASSCF(6,6)/HW(d). Geometric data are from the CASSCF results.

So, direct energy comparisons against one dimer calculation adopting model **1a** are not possible. Instead, the [2 + 2] cycloaddition channel on one dimer was recalculated using SIMOMM model **1b**, which serves as the reference energy (see Chart 7). The reaction barrier of **TS10** is calculated to be 3.8 kcal/mol, which is 6.0 kcal/mol lower than that of **TS1**. Such a discrepancy is due to the different computational theories.

According to the one dimer calculations, the [2 + 2] cycloaddition channel is much more favorable than direct Cl insertion channels. Therefore, the corresponding [2 + 2] cycloaddition channel was explored (see Chart 8). The [2 + 2] cycloaddition transition state of along the dimer row, **TS11**, connects the reactant **R2** and a diradical intermediate **I4** with a reaction barrier of 7.6 kcal/mol, which is 3.8 kcal/mol higher than that of **TS10**. Therefore, the [2 + 2] along the dimer row is slightly less favorable than that on the single dimer. The strong radical character of **TS11** can be easily seen from the NOON values of the CASSCF active space, which are 1.980, 1.976, 1.970, 1.959, 1.531, 1.045, 0.956, 0.470, 0.041, 0.030, 0.026, and 0.017.

Since the resulted intermediate **I4** still has a diracial character, it is less stable than the regular [2 + 2] cycloaddition product **R2** by 18.6 kcal/mol. In order to be stabilized, two chlorines are forming Cl7−C6 and Cl8−Si3 interactions in **I4**. By migrating Cl8 from C6 to Si3 and Cl7 from C5 to C6, the transition state **TS12** connects **I4** and stable and much less radical intermediate **I5**, which is more stable than the separated reactant by 44.6 kcal/mol. Again, by migrating Cl7 from C6 to Si2 and breaking Si1−C5 and Si1−Si2 bonds, the transition state **TS13** connects **I5** and stable intermediate **I6**, which is more stable than the separated reactant by 71.9 kcal/mol. Finally, the dichlorinated product **PCl5** is formed passing through transition state **TS14** with a mild barrier of −81.1 kcal/mol, by reforming the Si2−Si4 bond and breaking the Si2−C5 bond. The final

dichlorinated product **PCl5** is stable by 99.8 kcal/mol, which is as stable as the corresponding dichlorinated product **PCl4** on a single dimer.

D. Adsorptions Across the Dimer Rows. For the study of adsorptions across the dimer row, SIMOMM model **1c** was used in combination with (6,6) active space and HW(d) basis sets. Therefore, as in the case of along the dimer row calculations, the [2 + 2] cycloaddition channel on one dimer was recalculated using SIMOMM model **1c**, which serves as the reference energies (see Chart 9). The reaction barrier of **TS15** is calculated to be 3.4 kcal/mol, which is 5.6 kcal/mol lower than that of **TS1**. Such a discrepancy is due to the different computational theories.

The [2 + 2] cycloaddition reaction of across the dimer row is presented in Chart 10. Only one transition state **TS16** exists along this reaction pathway, directly connecting the reactant **R3** and the [2 + 2] cycloaddition product **P4**. The NOON values of CASSCF active space are 1.980, 1.497, 1.003, 0.997, 0.503, and 0.020 shows the diradical character of **TS16**. The reaction barrier of **TS16** is calculated to be 18.6 kcal/mol, which is 15.2 kcal/mol higher than that of [2 + 2] cycloaddition transition states **TS15**. Furthermore, product **P4** is less stable than the other [2 + 2] cycloaddition products **P3** by 12.4 kcal/mol. As a result, the [2 + 2] cycloaddition across the dimer row is both thermodynamically and kinetically less favorable than that on the single dimer.

IV. Conclusions

Multireference wave functions were used to study *trans*-1,2-dichloroethylene (DCE) absorption reactions on Si(100). As in the case of pristine ethylene, a diradical as well as a π-complex channel leading to [2 + 2] cycloaddition products were found. While chlorine substitution as compared to pristine ethylene facilitates the diradical path, the same substitution hinders the π-complex channel making the diradical path much more favorable between the two channels. Furthermore, the chlorine substitution simplifies the diradical pathway making it stereospecific, contrasting to the pristine ethylene mechanism.

Diradical [2 + 2] reaction channels and subsequent surface reactions along and across dimer rows were also explored. The [2 + 2] reaction on a single dimer is both kinetically and thermodynamically the most favorable. The same reactions along the dimer low are the second most favorable.

The major consequences of chlorine substitution as compared to the pristine ethylene reactions come from the new low-energy pathways to mono- and dichlorinated surface species, which are thermodynamically much more stable than the initial [2 + 2] product. However, it has been pointed out that the new pathways to chlorinated adstructures are not via direct C−Cl bond activation but via *indirect* isomerizations from the initial [2 + 2] products. So the direct reaction competitions between the [2 + 2] product and the chlorinated products do not exist. The combination of the low-energy surface isomerization channels and the thermodynamic stabilities make the chlorinated adstructures the major surface products, which is consistent with experimental observations. Consequently, the overall surface reactions become thermodynamically controlled.

Therefore, it is clear that substitutions not only affect the existing reaction channels but also introduce new reaction pathways, which may eventually determine the final surface products.

Acknowledgment. This work was supported by the Korea Research Foundation Grant funded by Korea Government (MOEHRD, Basic Research Promotion Fund) (KRF-2005-070-C00065).

References and Notes

(1) Woodward, R. B.; Hoffmann R. *The Conservation of Orbital Symmetry*; Verlag Chemie: Weinheim, 1970.

(2) (a) Nishijima, M.; Yoshinobu, J.; Tsuda, H.; Onchi, M. *Surf. Sci.* **1987**, *192*, 383. (b) Yoshinobu, J.; Tsuda, H.; Onchi, M.; Nishijima, M. *J. Chem. Phys.* **1987**, *87*, 7332. (c) Taylor, P. A.; Wallace, R. M.; Cheng, C. C.; Weinberg, W. H.; Dresser, M. J.; Choyke, W. J.; Yates, J. T., Jr. *J. Am. Chem. Soc.* **1992**, *114*, 6754. (d) Li, L.; Tindall, C.; Takaoka, O.; Hasegawa, Y.; Sakurai, T. *Phys. Rev. B* **1997**, *56*, 4648.

(3) (a) Imamura, Y.; Morikawa, Y.; Yamasaki, T.; Nakasuji, H. *Surf. Sci.* **1995**, *341*, L1091. (b) Liu, Q.; Hoffmann, R. *J. Am. Chem. Soc.* **1995**, *117*, 4082.

(4) (a) Waltenburg, H. N.; Yates, J. T., Jr. *Chem. Rev.* **1995**, *95*, 1589. (b) Choi, C. H.; Gordon, M. S. *Theoretical Studies of Silicon Surface Reactions with Main Group Absorbates*, Curtiss, L. A.; Gordon, M. S., Eds.; Kluwer Academic Publishers: Dordrecht; Chapter 4, pp 125−190; 2004.

(5) Wang, Y.; Ma, J.; Inagaki, S.; Pei, Y. *J. Phys. Chem. B* **2005**, *109*, 5199–5206.

(6) Lu, X.; Zhu, M.; Wang, X. *J. Phys. Chem. B* **2004**, *108*, 7359.

(7) Liu, H.; Hamers, R. J. *J. Am. Chem. Soc.* **1997**, *119*, 7593.

(8) Lopinski, G. P.; Moffatt, D. J.; Wayner, D. D. M.; Wolkow, R. A. *J. Am. Chem. Soc.* **2000**, *122*, 3548.

(9) (a) Becke, A. D. *J. Chem. Phys.* **1993**, *98*, 5648. (b) Stephens, P. J.; Devlin, F. J.; Chablowski, C. F.; Frisch, M. J. *J. Phys.Chem.* **1994**, *98*, 11623. (c) Hertwig, R. H.; Koch, W. *Chem. Phys. Lett.* **1997**, *268*, 345.

(10) (a) Lu, X. *J. Am. Chem. Soc.* **2003**, *125*, 6384. (b) Lu, X.; Zhu, M. *Chem. Phys. Lett.* **2004**, *393*, 124.

(11) Lee, H. S.; Choi, C. H.; Gordon, M. S. *J. Phys. Chem. B* **2005**, *109*, 5067.

(12) Hoffmann, H. M. R. *Angew. Chem., Int. Ed. Engl.* **1969**, *8*, 556.

(13) (a) Zhou, X. J.; Li, Q.; Leung, K. T. *J. Phys. Chem. B* **2006**, *110*, 5602. (b) Zhou, X. J.; He, Z. H.; Leung, K. T. *Surf. Sci.* **2006**, *600*, 468.

(14) Shoemaker, J. R.; Burgraff, L. W.; Gordon, M. S. *J. Phys. Chem. A* **1999**, *103*, 3245.

(15) (a) Allinger, N. L.; Yuh, Y. H.; Lii, J. H. *J. Am. Chem. Soc.* **1989**, *111*, 8551. (b) Lii, J. H.; Allinger, N. L. *J. Am. Chem. Soc.* **1989**, *111*, 8566. (c) Lii, J. H.; Allinger, N. L. *J. Am. Chem. Soc.* **1989**, *111*, 8576.

(16) Hehre, W. J.; Ditchfield, R.; Pople, J. A. *J. Chem. Phys.* **1972**, *56*, 2257.

(17) Hay, P. J.; Wadt, W. R. *J. Chem. Phys.* **1985**, *82*, 270.

(18) (a) Choi, C. H.; Gordon, M. S. *J. Am. Chem. Soc.* **1999**, *121*, 11311. (b) Choi, C. H.; Gordon, M. S. *The Chemistry of Organic Silicon Compounds*; Rappoport, Z.;. Apeloig, Y., Eds.; John Wiley & Sons: New York, 2001; Vol. 3; Chapter 15, pp 821−852. (c) Choi, C. H.; Gordon, M. S. Theoretical Studies of Silicon Surface Reactions with Main Group Absorbates, In *Computational Materials Chemistry: Methods and Applications*; Curtiss, L. A., Gordon, M. S., Eds.; Kluwer Academic Publishers: Dordrecht, 2004; Chapter 4, pp 125−190.

(19) (a) Sunberg, K. R.; Ruedenberg, K. In *Quantum Science*; Calais, J. L., Goscinski, O., Linderberg, J., Ohrn, Y., Eds.; Plenum: New York, 1976. (b) Cheung, L. M.; Sunberg, K. R.; Ruedenberg, K. *Int. J. Quantum Chem.* **1979**, *16*, 1103. (c) Ruedenberg, K.; Schmidt, M.; Gilbert, M. M.; Elbert, S. T. *Chem. Phys.* **1982**, *71*, 41. (d) Roos, B. O.; Taylor, P.; Siegbahn, P. E. *Chem. Phys.* **1980**, *48*, 157. (e) Schmidt, M. W.; Gordon, M. S. *Annu. Rev. Phys. Chem.* **1998**, *49*, 233.

(20) (a) Werner, H.-J. *Mol. Phys.* **1996**, *89*, 645. (b) Schmidt, M. S.; Gordon, M. S. *Annu. Rev. Phys. Chem.* **1998**, *49*, 233. (c) Glaesemann, K. R.; Gordon, M. S.; Nakano, H. *Phys. Chem. Chem. Phys.* **1999**, *1*, 967.

(21) (a) Nakano, H. J. *Chem. Phys.* **1993**, *99*, 7983. (b) Nakano, H. *Chem. Phys. Lett.* **1993**, *207*, 372.

(22) (a) Schmidt, M. W.; Baldridge, K. K.; Boatz, J. A.; Elbert, S. T.; Gordon, M. S.; Jensen, J. H.; Koseki, S.; Matsunaga, N.; Nguyen, K. A.; Su, S.; Windus, T. L.; Dupuis, M.; Montgomery, J. A., Jr. *J. Comput. Chem.* **1993**, *14*, 1347. (b) Fletcher, G. D.; Schmidt, M. W.; Gordon, M. S. *Adv. Chem. Phys.* **1999**, *110*, 267.

(23) Choi, C. H.; Gordon, M. S. *J. Am. Chem. Soc.* **2002**, *124*, 6162.

JP076526O